Field-induced charge separation dynamics in monolayer MoS_2

Daniele Vella,[1,2,3] Dmitry Ovchinnikov,[4,5] Daniele Viola,[6] Dumitru Dumcenco,[4,5] Yen C. Kung,[4,5] Eva A. A. Pogna,[6] Stefano Dal Conte,[6] Victor Vega-Mayoral,[1,2,7] Tetiana Borzda,[1,2] Matej Prijatelj,[1,2] Dragan Mihailovic[1,2] Andras Kis,[4,5] Giulio Cerullo,[6,8] and Christoph Gadermaier*[1,2]*

[1]Department of Complex Matter, Jozef Stefan Institute, Jamova 39, 1000 Ljubljana, Slovenia.

[2]Jozef Stefan International Postgraduate School, Jamova 39, 1000 Ljubljana, Slovenia.

[3]Department of Physics, National University of Singapore, 2 Science Drive 3, Singapore 117542, Singapore

[4]Electrical Engineering Institute, École Polytechnique Fédérale de Lausanne, CH-1015 Lausanne, Switzerland.

[5]Institute of Materials Science and Engineering, École Polytechnique Fédérale de Lausanne, CH-1015 Lausanne, Switzerland.

[6]Dipartimento di Fisica, Politecnico di Milano, Piazza Leonardo da Vinci 32, I-20133 Milano, Italy.

[7]School of Physics, Trinity College Dublin, Dublin 2, Ireland.

[8]Istituto di Fotonica e Nanotecnologie (IFN), CNR, Piazza Leonardo da Vinci 32, I-20133 Milano, Italy.

KEYWORDS excitons, transition metal dichalcogenides, femtosecond spectroscopy, photophysics, photovoltaics

ABSTRACT The absorption spectra of 2D semiconductors are dominated by excitons with binding energy of several hundreds of meV. Nevertheless, even single layers show an appreciable photovoltaic effect and work as the active material in high sensitivity photodetectors, thus indicating some degree of free charge carrier photogeneration. Here, we perform ultrafast transient absorption spectroscopy on monolayer MoS_2 in a field-effect transistor configuration. We show that even a moderate in-plane electric field of a few $kVcm^{-1}$ can significantly increase the yield of charge carriers from photogenerated hot electron-hole pairs.

Introduction

In the past few years, layered two-dimensional semiconductors such as transition metal dichalcogenides (TMDCs) moved into the focus of optoelectronics and nanophotonics research due to their exceptionally strong light-matter interaction combined with flexible processing and fabrication[1-3] and intense nonlinear optical response.[4-6] Charge carrier photogeneration is the enabling step for photovoltaics and photodetectors. However, photoexcitation in TMDCs generates excitons with significant, thickness-dependent binding energy, reaching 400-700 meV in the monolayer case.[7-9] Hence, efficient photovoltaic and photodetector devices require measures

to facilitate exciton dissociation into charge carriers, such as a vertical donor-acceptor heterostructure or an engineered p-n junction.[10-15]

In few-layer MoS_2 and WS_2 with exciton binding energies similar to the bulk values (50-150 meV)[16] excitation well above the A and B resonances creates hot electron-hole pairs (C excitons at the band nesting region[17] and/or charge carriers in the continuum of valence and conduction band states). Upon relaxation towards the relative band maxima/minima, they can either separate into free charge carriers or form A excitons, which give rise to excitonic photoluminescence (PL). In the few-layer case, separation into free carriers with a time constant of approximately 1 ps is the dominant process[18-23] while in the monolayer case, due to the larger binding energy, a significant fraction of A excitons are formed.[17, 24-26] However, the observed photovoltaic effect and photocurrent suggest that, even if to a lesser extent, charge carriers form also in monolayers. The PL quantum yield of monolayer MoS_2 decreases as the excitation photon energy increases[17,24], indicating that also in the monolayer hot electron-hole pairs can separate into free charge carriers.

Here, to gain further insight into the charge generation mechanism, we propose to modulate its efficiency by applying an electric field.[27] We use monolayer MoS_2 as the channel of a field-effect transistor (FET) and apply an in-plane electric field via the source-drain voltage. We first show that the PL of MoS_2 is progressively quenched upon the application of increasingly strong in-plane electric fields. Subsequently, we perform femtosecond optical pump-probe microspectroscopy to directly monitor the fate of the photogenerated hot electron-hole pairs and the carriers arising from their dissociation. For increasing field strengths, we observe an enhanced formation of carriers during the first few ps. Both findings suggest that the electric field facilitates the separation of photogenerated charge pairs. The temporal evolution of the charge density provides insight into the separation mechanism.

Results and Discussion

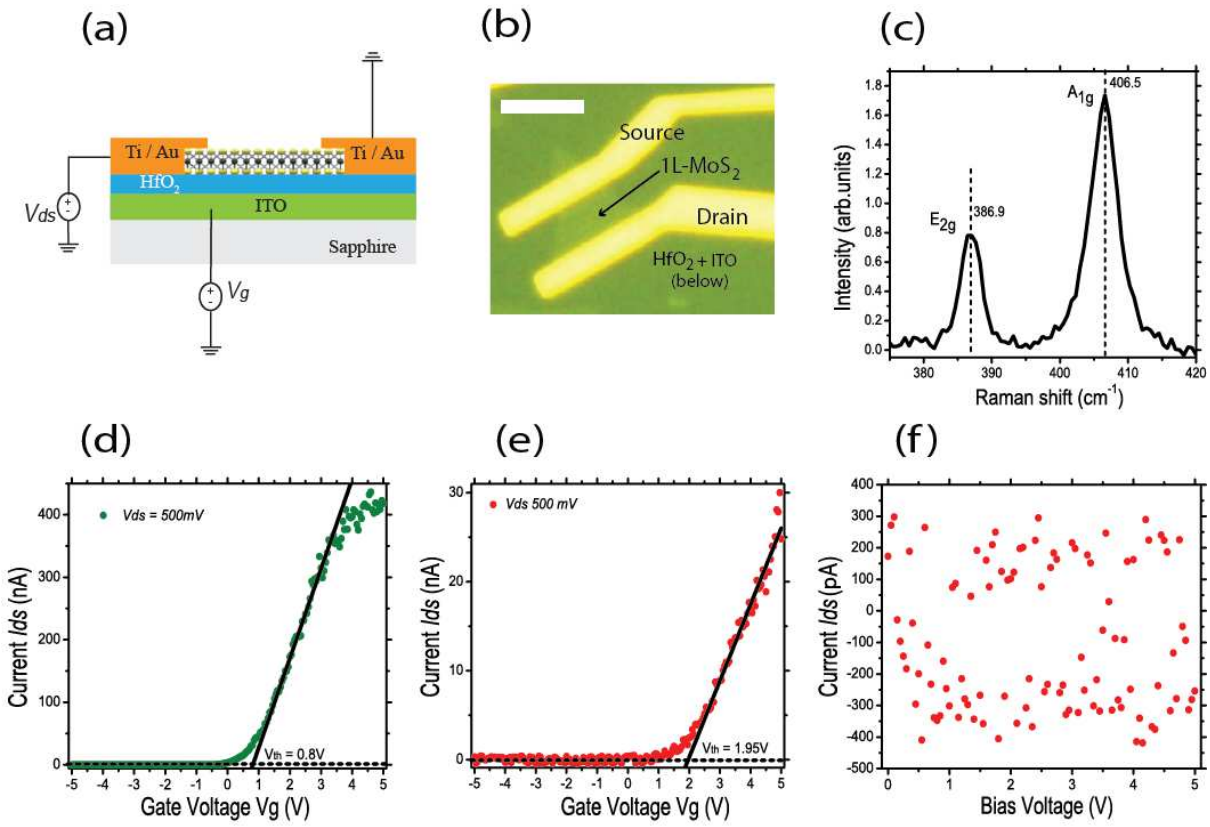

Figure 1. (a) Schematic illustration of the transparent field effect transistor. **(b)** Optical image of the device. Scale bar is 10 µm. **(c)** Raman modes of the single layer MoS_2. **(d)** Transfer characteristic (Ids-Vg) of the device immediately after the microfabrication process. **(e)** Transfer characteristic recorded before the optical measurements. **(f)** Output characteristic recorded before the optical measurements, showing negligible charge injection (for Vg = 0 V).

Figure 1 shows a schematic drawing (Fig. 1a) and an optical microscope image (Fig. 1b) of the FET structure used in this study. The transistor is built in a bottom-gate configuration, using sapphire as the transparent substrate and 50 nm of indium tin oxide (ITO) as the transparent back-

gate electrode, thus enabling optical measurements in transmission geometry. The gate dielectric consists of 30 nm of HfO_2 (ε_r = 19). Figure 1c shows the Raman spectrum of the chemical vapor deposition (CVD) MoS_2 flake; the distance $\Delta\omega$ = 19.6 cm^{-1} between the A_{1g} and the E^1_{2g} peaks confirms the monolayer thickness.[28] Figures 1d and 1e present the transfer characteristics of the device immediately after fabrication and at the time of transient absorption measurements. The increase in turn-on voltage (V_{on}) from 0.8 V to 1.95V is ascribed to adsorption doping since the measurements are carried out in air.[29] Source-drain voltages V_{ds} up to 5V (at V_g = 0 V, used throughout all experiments) are possible without appreciable charge injection, as shown in Fig. 1f. This allows to observe the isolated effect of field-induced charge photogeneration without signal contributions from injected charges.

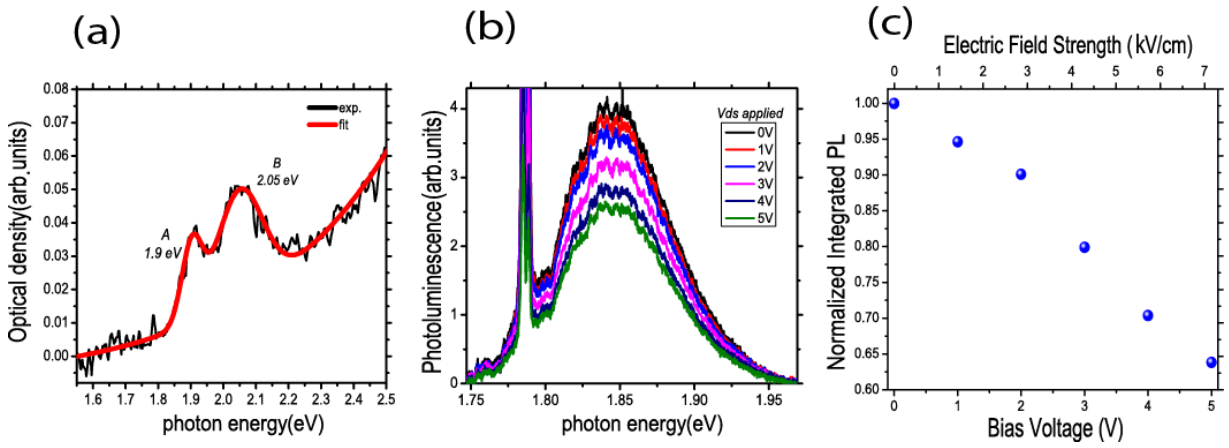

Figure 2. (a) Extinction spectrum of the MoS_2 monolayer (black curve). Fit by using two Gaussian peaks and a generic exponential function to account for the background from various scattering mechanisms. **(b)** PL spectra for different bias voltages applied. The feature at 1.78 eV comes from the incomplete subtraction of the sapphire substrate fluorescence **(c)** Normalized integrated PL as a function of the electric field strength.

The PL spectrum of monolayer MoS_2 upon photoexcitation at 2.54 eV, displayed in Fig. 2b, shows one main feature around 1.85 eV,[24,25] slightly red-shifted compared to the A exciton resonance in absorption[30,31] (Figure 2a). The shape of this feature suggests two overlapping peaks, one from neutral excitons A^0 and one from charged trions A^- due to the doping of the sample.[9,29,30,32,33] If we apply an in-plane electric field via the source-drain voltage, the PL intensity progressively decreases as the field increases. For the highest bias used, V_{ds} = 5 V, which corresponds to an electric field of 7 $kVcm^{-1}$ (the distance between the electrodes is 7 μm), the PL is quenched by about 35 % (Figure 2c). The field-induced PL quenching is weaker than that observed in heterostructures such as MoS_2/WSe_2,[11,34] where the integrated PL at the heterojunction decreases, respectively, by 81% and 98% compared to isolated MoS_2 and WSe_2 monolayers. In the heterojunction the band alignment promotes the charge separation and the charge transfer mechanism is faster than any other radiative or non-radiative decay channel. The field-induced PL quenching observed here can in principle have two different origins: either the A excitons and trions, which give rise to PL, have a certain field-enhanced possibility to dissociate during their lifetime, or the field modifies the branching ratio between bound states (A excitons and trions) and free carriers during the initial relaxation of hot charge pairs.

In order to resolve the temporal dynamics of the field-induced charge generation we employed electric-field-assisted pump-probe microspectroscopy. The microscope is built in collinear geometry (Figure 3a). A broadband white light probe is focused by a reflective microscope objective onto a spot of ~800 nm diameter. By using a piezo-nanopositioner we scan the sample in the probe beam focus. Once the area of interest is selected, the probe is centered inside the FET channel and a pump pulse is successively focused onto the sample collinearly with the probe (spot

size 5 times bigger than the probe). To allow some degree of charge photogeneration even in the absence of an electric field and to facilitate a comparison with previous studies,[18-22] we use the customary pump pulse photon energy of 3.1 eV, well above the electronic bandgap of MoS_2, where we expect a branching between the formation of excitons and free carriers already without electric field.[17] In order to keep re-excitation or de-excitation by the probe at negligible levels, the probe fluence is kept much lower than the pump fluence.

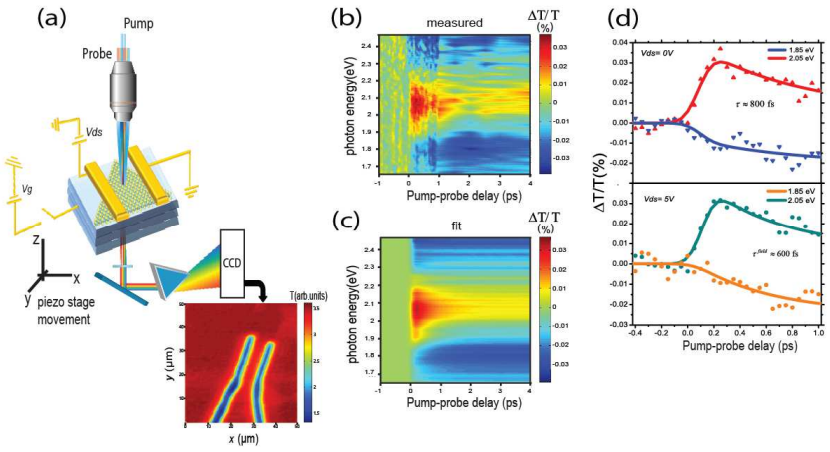

Figure 3. (a) Schematic illustration of the pump-probe microscope setup. **(b)** The measured transient transmission contour plot as a function of the probe photon energy and pump-probe delay (at 5 V). **(c)** Simulated transient transmission contour plot according to the model described in the text. **(d)** Dynamics at 1.85 and 2.05 eV with (bottom-panel) and without field (top-panel). Points: experimental data. Solid lines: fits according to the model described in the text.

The transient relative change in transmission $\Delta T/T$ is directly related to the photoinduced change in the absorbance:

$$\frac{\Delta T}{T} \approx -\Delta\alpha(\omega, t)d \quad (1)$$

with $\alpha(\omega)$ the absorption coefficient and *d* the sample thickness. The absorption coefficient

can be expressed as the product of the density of absorbers *n* and their absorption cross-section $\sigma(\omega)$: $\alpha(\omega) = \sum_i \left(n_i \sigma_i(\omega)\right)$ so that its time-dependent change becomes:

$$\Delta\alpha(\omega, t) = \sum_i \left(\sigma_i(\omega, t)\Delta n_i(t) + n_i(t)\Delta\sigma_i(\omega, t)\right) \quad (2)$$

In most cases, the first term in Equation (2) dominates and the signal dynamics follows the evolution of excited states' populations. However, Stark effect due to photogenerated charges[35], the Burstein-Moss effect,[36] and, in particular, band-gap renormalization[37] may induce an appreciable change in the absorption cross-section, leading to a non-negligible second term. Nevertheless, in all three mechanisms the effect is due to the presence of photoexcited states, hence, $\Delta\sigma$ should also follow their population. It is therefore justified to assume that the $\Delta T/T$ signal evolution follows the photoexcited states' population dynamics.

Figure 3b shows the 2D ΔT/T plot as a function of the probe photon energy and pump-probe delay. The spectra show two photoinduced absorption (PA) features (negative signal at the spectral windows around 2.4eV and 1.8eV) and a photobleaching (PB) peak (positive signal) in correspondence of the excitonic resonances A and B which, for excitation at 3.1 eV, tend to merge in a single peak[37]. The PB rises with the instrumental response function (pump-probe cross-correlation) and decays and narrows with increasing delay. The two PA features also form immediately, but continue to grow and to broaden. Such behavior suggests that the signal originates from at least two distinct excited state populations, a primary one that is directly created by photoexcitation, and a secondary one that forms from the relaxation of the former. The primary

population are the hot electron-hole pairs created by photoexcitation, while the secondary one is an ensemble of excitons, trions and free carriers, in unquantified proportion.

Figure 3d shows the time evolution of the signal at two selected probe photon energies: the PB at 2.05 eV, which forms within the time resolution of the instrument and decays rapidly, and the PA at 1.85eV which shows a delayed formation after the initial rise. Both the PB decay and the PA formation can be fitted as a single-exponential process with a time constant of 800 fs, which is very similar to the 700 fs reported for multilayers[18] and is indicative of the time scale for the relevant relaxation processes of hot charge pairs into A excitons and free carriers.

To model the signal over the first few picoseconds, we describe the time-dependent populations in Equation 2 by a system of rate equations. We assume that photoexcitation creates a primary population *P(t)* of hot electron-hole pairs. *P(t)* evolves into a secondary population *S(t)* of excitons and free carriers with a time constant $\tau_1 = 1/k_1$:

$$\frac{dP}{dt} = G(t) - k_1 P$$

$$\frac{dS}{dt} = +k_1 P \qquad (3)$$

with $G(t)$ the generation term (pump-probe cross-correlation, approximated as a Gaussian). This simple model reproduces the data very well (Figure 3c) with a time constant $\tau_1 = 800$ fs.

The spectral contributions of the ensemble populations *P(t)* and *S(t)* are shown in Figure 4a. The main difference is that *S(t)* has a weaker and narrower PB and a stronger and broader PA on the low-energy side. Figure 4b shows the population dynamics, which is well described by the evolution of one ensemble into the other during the relaxation with a time constant τ_1. As has been shown recently,[37] the excitation of hot electron-hole pairs does not immediately change the

occupation of the states relevant for the A and B absorption peak. The $\Delta T/T$ signal immediately after photoexcitation is dominated by the second term of Equation (2) due to a combination of band gap renormalization and screening of the exciton binding energy, which leads to a spectral shift of the absorption spectra. Subsequently, the relaxation towards excitons and trions as well as free charges changes the relevant states' population and the first term of Equation (2) becomes more important for the $\Delta T/T$ signal. Its most dominant features are the bleaching of the excitonic transitions and the PA feature below 1.9 eV due to free carriers.[18,19,21]

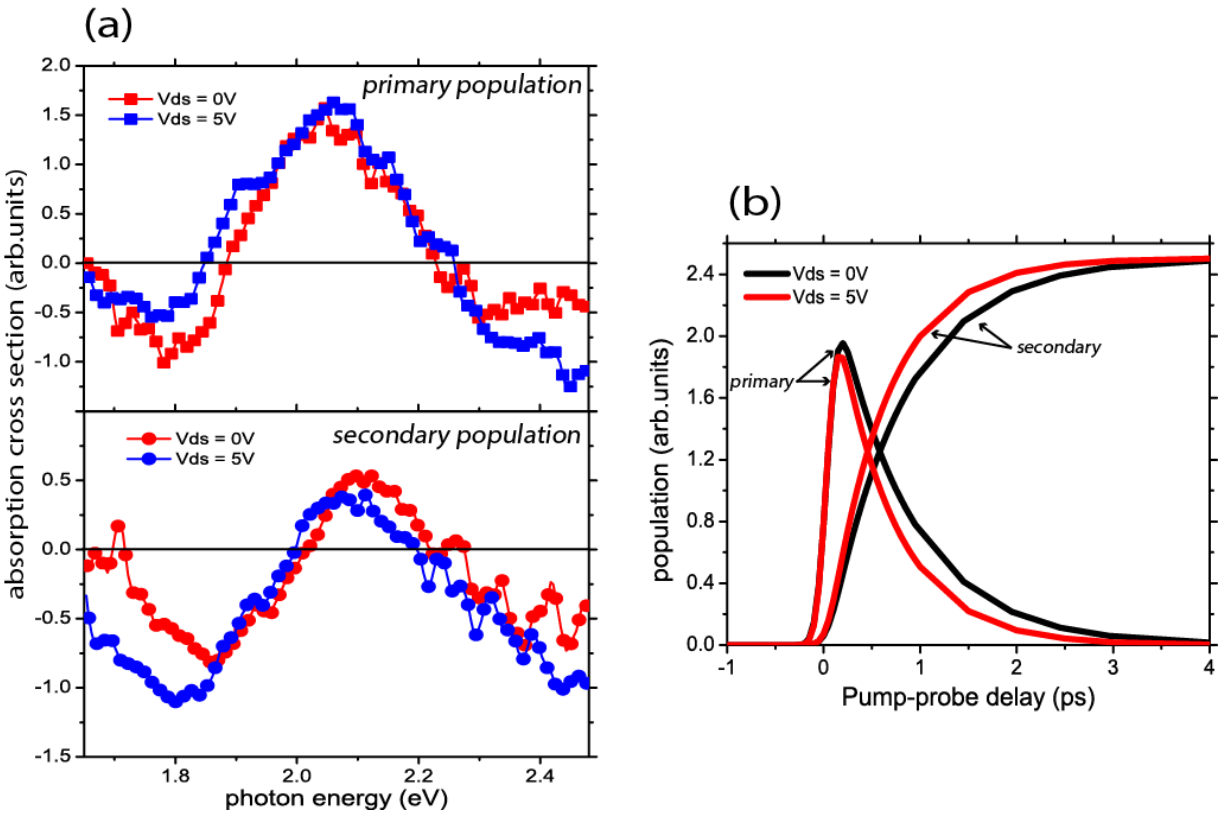

Figure 4. (a) Spectral contributions of primary (top panel) and secondary (bottom panel) populations with and without electric field. **(b)** Time dependent primary and secondary populations with and without electric field.

Upon applying an in-plane electric field of 7kVcm^{-1}, as in the PL quenching experiments, τ_1 reduces to 600 fs (Fig. 4b) and the difference between the spectra of the ensembles *P(t)* and *S(t)* becomes more pronounced (Fig. 4a): the PB of *S(t)* is weaker and the low energy PA is stronger than in the absence of electric field. This suggests that the applied field increases the concentration of charges in the ensemble *S(t)* by enhancing the charge separation yield.

To further illustrate the differences in the evolution of the $\Delta T/T$ spectrum with and without the electric field we now consider the field-induced spectrum $\Delta^2 T/T$ defined as the difference of the $\Delta T/T$ spectra in the presence and in the absence of an electric field:

$$\frac{\Delta^2 T}{T}(\omega, t) = \frac{\Delta T}{T}(\omega, t)_{field} - \frac{\Delta T}{T}(\omega, t) = -d \sum_i [\Delta_F n_i(t)]\, \sigma_i(\omega) - d \sum_i n_i(t) [\Delta_F \sigma_i(\omega)] \qquad (4)$$

The first term in Eq. (4) describes field-induced changes (indicated with Δ_F in the equation) in the excited state populations while the second term indicates field induced changes (Δ_F) in the absorption cross section (Stark shift of the excited state[38,39]). The most important effect of the electric field is an increase of the PA of the secondary population over the energy interval 1.65-1.85 eV (Figure 5a). This increase is of similar magnitude as the $\Delta T/T$ signal itself, pointing towards a sizable increase in the charge density due to field-induced charge separation. The temporal evolution of this signal, integrated over the energy interval 1.65-1.85 eV, is shown in Figure 5b. Initially, when the amount of extra charges is negligible, the signal is positive, since it is dominated by the red-shifted PB of excitons, attributed to the Stark effect, seen in Figure 4a. Gradually, as the field-induced population of charges builds up over a few ps, their PA starts to dominate the whole spectral window.

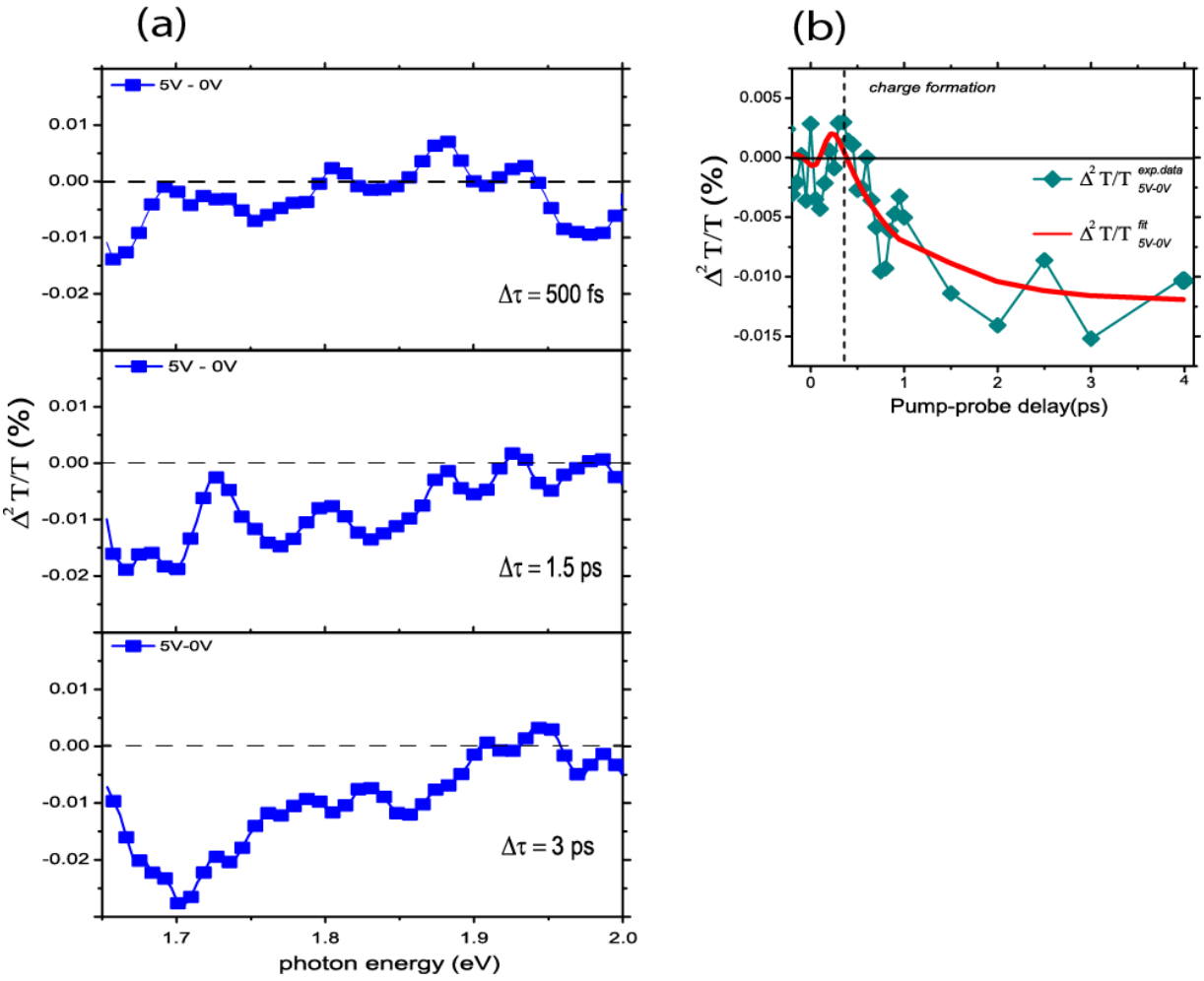

Figure 5. (a) Δ^2T/T spectral feature for three different delays (0.5, 1.5, 3 ps). **(b)** Temporal evolution of the absorption feature, observed in the Δ^2T/T signal, averaged over the energy interval 1.65 - 1.85 eV.

From the field-induced PL quenching together with the field-induced enhancement of the charge contribution to the $\Delta T/T$ signal, we can now develop a scenario of the photoexcitation dynamics in monolayer MoS_2 and related materials in the presence of an electric field. Photoexcitation with a photon energy above the A and B exciton resonances creates hot electron-hole pairs. “Hot” in

this context means that to relax towards the lowest excited state – the A exciton – multiple electron-phonon scattering processes are necessary. We find a characteristic time scale of 600-800 fs for this relaxation. At the end of this relaxation process we have a Coulombically interacting electron-hole pair with a certain spatial separation r_i as the result of the multiple scattering events. As commonly described by the Onsager theory of geminate recombination, [40-42] this electron-hole pair can either coalesce into an exciton or the two carriers can separate in a random walk driven by scattering with the phonon bath. The branching ratio depends on the available phonons – and hence on the sample temperature and the excess energy of the exciting phonon, and on the initial separation. An applied electric field can both increase the separation and also tilt the Coulombic potential, making the separation more favorable. The combined action of these processes shifts the branching ratio towards charge separation, resulting in a lower PL quantum yield and a stronger yield of photogenerated charges.

Conclusions

We have studied the optical response (PL and ultrafast transient absorption) of monolayer MoS_2 in the presence of an electric field. Our results show that a moderate electric field of a few $kVcm^{-1}$ can significantly modulate the branching between different relaxation paths for photogenerated hot electron-hole pairs in monolayer MoS_2: towards photoluminescent A excitons and trions on the one hand, and free carriers on the other. The electric field skews the ratio towards free carriers, suggesting a field-induced charge separation during the hot charge pair relaxation. For a subsequent dissociation of the relaxed excitons due to the distortion of the excitonic Coulomb potential, the in-plane field is too weak.[40,43] During the relaxation, the carriers undergo multiple scattering processes upon phonons and defects. In the course of this diffusive process, a certain

fraction of the charges form excitons or trions, while the others separate and contribute to the photocurrent. The electric field increases the average separation and enhances the photocurrent on the expense of PL. Due to this mechanism, a relatively modest electric field can increase the yield of charge carrier photogeneration and hence the efficiency of photodetectors and photovoltaic elements based on TMDC monolayers.

Materials and Methods

The transistor is built according to the structure in Ref 44, using c-plane sapphire as the transparent substrate and 50 nm of ITO as the transparent back-gate electrode. The gate dielectric consists of 30 nm of HfO_2 deposited by atomic layer deposition; the source and drain electrodes are made of Ti/Au (5/50nm thickness). Monolayer MoS_2 has been grown by CVD on c-plane sapphire following the method in Ref. 45. As-synthesized MoS_2 was transferred from the sapphire to the target substrate (sapphire/ITO/HfO_2) by using PMMA A2 as a support film and etching in 30% KOH as described in Ref. 45.

PL on the MoS_2 FET was measured with an NT-MDT NTEGRA SPECTRA confocal PL-Raman microscope in backscattering geometry. We used the excitation line at 488 nm and a 100X objective (N.A. 0.9) to focus onto a spot size of 2μm. The PL signals were detected with a CCD array at −80°C. We kept the laser intensity below 1kWcm^{-2}.

For the pump-probe measurements we use an amplified Ti:sapphire laser (Coherent Libra), emitting 100-fs pulses at 1.55 eV, with average power of 4 W at 2 kHz repetition rate. A 320 mW fraction of the laser power is used for our experiments. The output beam is divided by a 50/50

beam splitter into pump and probe lines. We produce ~100 fs pump pulses at 3.1 eV by second harmonic generation. The probe is obtained by white light continuum generation in a 5 mm-thick CaF_2 plate, filtering out light at the fundamental frequency with a colored glass short-pass filter. To have an imaging system the chip carrier is mounted on a translation stage made of two units, a motorized 2-axis translation stage for the coarse movement (resolution ~ 625 nm) and a 3-axis computer controlled piezoelectric translation stage (with 1 nm resolution) that allows better accuracy and to adjust the focus on the sample. With these two translation stages one can raster scan the sample in order to get an image. In order to have a high spatial resolution image by raster scanning the sample, we need to focus tightly both the pump and the probe beam on the sample. To achieve this, without losing temporal resolution and avoiding chromatic aberrations, we use a reflective objective with a 15X magnification and a 0.30 numerical aperture (NA) to focus pump and probe pulses in collinear geometry (see Figure 3a). Making the diameter of the probe beam bigger than the pump before the objective leads to the probe pulse with a sub-micrometer spot size on the sample and a pump pulse with a spot size ~5 times bigger. The transmitted probe is collected with a 7.5 mm achromatic doublet, dispersed by a CaF_2 prism and detected by a Si CCD camera with 532 pixels, corresponding to a bandwidth per pixel of 1.1 nm. In this way we obtain a 3D transmission map $T(x, y, \lambda)$ and differential transmission $\Delta T/T(x,y,\lambda,t)$ for a given position (x,y). Due to the tight focusing, we needed to use a very low probe intensity so as not to re-excite the sample. To increase the counts on the spectrometer and reduce the noise level, we worked with a chopper frequency of 125 Hz, always summing over eight consecutive pulses with probe on and off, respectively.

AUTHOR INFORMATION

Corresponding Author

*Authors to whom correspondence should be addressed: phydv@nus.edu.sg , christoph.gadermaier@ijs.si

Funding Sources

The research leading to these results has received funding from the Marie-Curie ITN "MoWSeS" (grant no. 317451),the European Union's Seventh Framework Programme FP7/2007-2013 under Grant Agreement No. 318804 (SNM), the Swiss SNF Sinergia Grant no. 147607, the European Union Horizon 2020 Programme under Grant Agreement No. 696656 Graphene Flagship, the Slovenian Research Agency programme P1-0040 and European Research Council advanced grant TRAJECTORY.

ACKNOWLEDGMENT

We thank V.V. Kabanov, V. Perebeinos, J. Strle, and N. Vujicic for stimulating discussions. Device fabrication was carried out in the EPFL Center for Micro/Nanotechnology (CMI). We thank Z. Benes (CMI) for technical support with e-beam lithography.

REFERENCES

[1] Wang, Q. H.; Kalantar-Zadeh, K.; Kis, A.; Coleman, J. N.; Strano, M. S. Electronics and optoelectronics of two-dimensional transition metal dichalcogenides, *Nat. Nanotechnol*. **2012**, 7, 699-710.

[2] Mak, K. F.; Shan, J. Photonics and optoelectronics of 2D semiconductor transition metal dichalcogenides. *Nat. Photon*. **2016**, 10, 216-226.

[3] Sun, Z.; Martinez, A.; Wang, F. Optical modulators with 2D layered materials, *Nat. Photon*. **2016**, 227-238.

[4] Wang, K. P. *et al*. Ultrafast Saturable Absorption of Two-Dimensional MoS_2 Nanosheets. *ACS Nano* **2013**, 7, 9260-9267.

[5] Zhang, H., Lu, S. B., Zheng, J., Du, J., Wen, S. C., Tang, D. Y., Loh, K. P. Molybdenum disulfide (MoS_2) as a broadband saturable absorber for ultra-fast photonics *Opt. Expr*. **2014**, 22, 7249-7260.

[6] Zhang, S. F. *et al*. Direct Observation of Degenerate Two-Photon Absorption and Its Saturation in WS_2 and MoS_2 Mono layer and Few-Layer Films. *ACS Nano* **2015**, 9, 7142-7150.

[7] Ye, Z.; Cao, T.; O'Brien, K.; Zhu, H.; Yin, X.; Wang, Y.; Louie, S., G.; Zhang, X. Probing excitonic dark states in single-layer tungsten disulphide, *Nature* **2014**, 513, 214-218.

[8] Chernikov, A.; Berkelbach, T. C.; Hill, H. M.; Rigosi, A.; Li, Y.; Aslan, O. B.; Reichman, D. R.; Hybertsen, M. S.; Heinz, T. F. Exciton binding energy and non-hydrogenic Rydberg series in monolayer WS_2, *Phys. Rev. Lett*. **2014**, 113, 076802.

[9] Chernikov, A.; van der Zande, A. M.; Hill, H. M;. Rigosi, A. F.; Velauthapillai, A.; Hone, J.; Heinz, T. F. Electrical tuning of exciton binding energies in monolayer WS_2, *Phys. Rev. Lett.* **2015**, 115, p. 126802.

[10] Fontana, M.; Deppe, T.; Boyd, A. K.; Rinzan, M.; Amy, M. P.; Liu, Y.; Barbara, P. Electron-hole transport and photovoltaic effect in gated MoS_2 Schottky junctions, *Sci. Rep*. **2013**, 3, 1634.

[11] Lee, C.-H.; Lee, G.-H.; van der Zande, A. M.; Chen, W.; Li, Y.; Han, M.; Cui, X.; Arefe, G.; Nuckolls, C.; Heinz, T. F.; Guo, J.; Hone, J.; Kim, P. Atomically thin p-n junctions with van der Waals heterointerfaces. *Nat. Nanotechnol*. **2014**, 676-681.

[12] Lopez-Sanchez, O.; Llado, E. A.; Koman, V.; Morral, A. F. I.; Radenovic, A.; Kis, A. Light generation and harvesting in a van der Waals heterostructure, *ACS Nano* **2014**, 8, 3042-3048.

[13] Baugher, B. W. H.; Churchill, H. O. H.; Yang, Y.; Jarillo-Herrero, P. Intrinsic electronic transport properties of high-quality monolayer and bilayer MoS_2. *Nano Lett.* **2013**, 13, 4212-4216.

[14] Pospischil, A.; Furchi, M. M.; Mueller, T. Solar-energy conversion and light emission in an atomic monolayer p-n diode. *Nat. Nanotechnol*. **2014**, 9, 257-261.

[15] Britnell, L.; Ribeiro, R. M.; Eckmann, A.; Jalil, R.; Belle, B. D.; Mishchenko, A.; Kim, Y.-J.; Gorbachev, R. V.; Georgiou, T.; Morozov, S. V.; Grigorenko, A. N.; Geim, A. K.; Casiraghi, C.; Castro Neto, A. H.; Novoselov, K. S. Strong light-matter interactions in heterostructures of atomically thin films. *Science* **2013**, 340, pp. 1311-1314.

[16] Evans, B. L.; Young, P. A.; Exciton spectra in thin crystals: the diamagnetic effect. *Proc. Phys. Soc.* **1967**, 91, 475-482.

[17] Kozawa, D.; Kumar, R.; Carvalho, A.; Amara, K. K.; Zhao, W.; Wang, S.; Toh, M.; Ribeiro, R. M.; Castro Neto, A. H.; Matsuda, K.; Eda, G. Photocarrier relaxation pathway in two-dimensional semiconducting transition metal dichalcogenides. *Nat. Commun*. **2014**, 5, 4543.

[18] Borzda, T.; Gadermaier, C.; Vujicic, N.; Topolovsek, P.; Borovsak, M.; Mertelj, T.; Viola, D.; Manzoni, C.; Pogna, E. A. A.; Brida, D.; Antognazza, M. R.; Scotognella, F.; Lanzani, G.; Cerullo, G.; Mihailovic, D. Charge photogeneration in few-layer MoS_2. *Adv. Funct. Mater*. **2015**, 25, 3351-3358.

[19] Vega-Mayoral, V.; Vella, D.; Borzda, T.; Prijatelj, M.; Tempra, I.; Pogna, E. A. A.; Dal Conte, S.; Topolovsek, P.; Vujicic, N.; Cerullo, G.; Mihailovic, D.; Gadermaier, C. Exciton and charge carrier dynamics in few-layer WS_2. *Nanoscale*, **2016**, 8, 5428-5434.

[20] Cunningham, P. D.; McCreary K. M.; Hanbicki, A. T.; Currie, M.; Jonker, B. T.; Hayden, L. M. Charge Trapping and Exciton Dynamics in Large-Area CVD Grown MoS_2. *J. Phys. Chem. C* **2016**, 120, 5819-5826.

[21] Tsokkou, D.; Yu, X.; Sivula, K.; Banerji, N. The role of excitons and free charges in the excited-state dynamics of solution-processed few-layer MoS_2 nanoflakes. *J. Phys. Chem. C* **2016**, 120, 23286-23292.

[22] Wang, L.; Wang, Zh.; Wang, H.-Y.; Grinblat, G.; Huang, Y.-L.; Wang, D.; Ye, X.-H.; Li, X.-B.; Bao, Q.; Wee, A. T.-S.; Maier S. A.; Chen, Q.-D.; Zhong, M.-L.; Qiu, C.-W.; Sun, H.-B. Slow cooling and efficient extraction of C-exciton hot carriers in MoS_2 monolayer. *Nat. Commun.* **2016**, 8, 13906.

[23] Ruppert, C.; Chernikov, A., Hill, H. M.; Rigosi, A. F.; Heinz, T. F. The Role of Electronic and Phononic Excitation in the Optical Response of Monolayer WS_2 after Ultrafast Excitation. *Nat. Commun.* **2016**, 8, 13906.
[24] Mak, K. F.; Lee, C.; Hone, J.; Shan, J.; Heinz, T. F. Atomically thin MoS_2: A new direct-gap semiconductor. *Phys. Rev. Lett*. **2010**, 105, 136805.
[25] Splendiani, A.; Sun, L.; Zhang, Y.; Li, T.; Kim, J.; Chim, C.-Y.; Galli, G.; Wang, F. Emerging photoluminescence in monolayer MoS_2. *Nano Lett*. **2010**, 10 1271-1275.
[26] Hill, H. M.; Rigosi, A. F.; Roquelet, C.; Chernikov, A.; Berkelbach, T. C.; Reichman, D. R.; Hybertsen, M. S.; Brus, L. E.; Heinz, T. F. Observation of excitonic Rydberg states in monolayer MoS_2 and WS_2 by photoluminescence excitation spectroscopy. *Nano Lett*. **2015**, 15, 2992-2997.
[27] Graupner, W.; Cerullo, G.; Lanzani, G.; Nisoli, M.; List, E. J. W.; Leising, G.; Silvestri, S. D. Direct observation of ultrafast field-induced charge generation in ladder-type poly(para-phenylene). *Phys. Rev. Lett*. **1998**, 81, 3259-3262.
[28] Lee, C.; Yan, H.; Brus, L. E.; Heinz, T. F.; Hone, J.; Ryu, S. Anomalous lattice vibrations of single- and few-layer MoS_2. *ACS Nano* **2010**, 4, 2695-2700.
[29] Yue, Q.; Shao, Z.; Chang, S.; Li, J. Adsorption of gas molecules on monolayer MoS_2 and effect of applied electric field. *Nanoscale Res. Lett*. **2013**, 8, 425.
[30] Mak, K. F.; He, K.; Lee, C.; Lee, G. H.; Hone, J.; Heinz, T. F.; Shan, J. Tightly bound trions in monolayer MoS_2, *Nat. Mater*. **2013**, 12, 207-211.
[31] Zhao, W.; Ghorannevis, Z.; Chu, L.; Toh, M.; Kloc, C.; Tan, P.-H.; Eda, G. Evolution of electronic structure in atomically thin sheets of WS_2 and WSe_2. *ACS Nano* **2013**, 7, 791-797, 2013.
[32] Sercombe, D.; Schwarz, S.; Pozo-Zamudio, O. D.; Liu, F.; Robinson, B. J.; Chekhovich, E. A.; Tartakovskii, I. I.; Kolosov, O.; Tartakovskii, A. I. Optical investigation of the natural electron doping in thin MoS_2 films deposited on dielectric substrates. *Sci. Rep*. **2014**, 3, 3489.
[33] Jones, A. M.; Yu, H.; Ghimire, N. J.; Wu, S.; Aivazian, G.; Ross, J. S.; Zhao, B.; Yan, J.; Mandrus, D. G.; Xiao, D.; Yao, W.; Xu, X. Optical generation of excitonic valley coherence in monolayer WSe_2. *Nat. Nanotechnol*. **2013**, 8, 634-638.
[34] Hong, X.; Kim, J.; Shi, S.-F.; Zhang, Y.; Jin, C.; Sand, Y.; Tongay, S.; Wu, J.; Zhang, Y.; Wang, F. Ultrafast charge transfer in atomically thin MoS_2/WS_2. *Nat. Nanotechnol*. **2014**, 9, 682-686.
[35] Gadermaier, C.; Menna, E.; Meneghetti, M.; Kennedy, W. J.; Vardeny, Z. V.; Lanzani, G. Long-Lived Charged States in Single-Walled Carbon Nanotubes. *Nano Lett*. **2006**, 6, 301-305.
[36] Sun, Q.-C.; Yadgarov, L.; Rosentsveig, R.; Seifert, G.; Tenne, R.; Musfeldt, J. L. Observation of a Burstein-Moss shift in rhenium-doped MoS_2 nanoparticles. *ACS Nano* **2013**, 7 3506-3511.
[37] Pogna, E. A. A.; Marsili, M.; De Fazio, D.; Dal Conte, S.; Manzoni, C.; Sangalli, D.; Yoon, D.; Lombardo, A.; Ferrari, A. C.; Marini, A.; Cerullo, G.; Prezzi, D. Photoinduced bandgap renormalization governs the ultrafast response of single-layer MoS_2. *ACS Nano* **2016**, 10, 1182-1188.
[38] Vella, D.; Ovchinnikov, D.; Martino, N.; Vega-Mayoral, V.; Dumcenco, D.; Kung, Y.-C.; Antognazza, M.-R.; Kis, A.; Lanzani, G.; Mihailovic, D.; Gadermaier, C. Unconventional Electroabsorption in Monolayer MoS_2. *2d Mater*. **2017**, 4, 021005.
[39] Gadermaier, C.; Grasse, F.; Perissinotto, S.; Graf, M.; Galbrecht, F.; Scherf, U.; List, E. J. W.; Lanzani, G. Stark spectroscopy of excited-state transitions in a conjugated polymer. *Phys. Rev. Lett*. **2008**, 100, 057401.
[40] Arkhipov, V. I.; Emelianova, E. V.; Bässler, H. Hot exciton dissociation in a conjugated polymer. *Phys. Rev. Lett*. **1999**, 82, 1321-1324.
[41] L. Onsager, Initial recombination of ions. *Phys. Rev*. **1938**, 54, 554-557.
[42] Pai D. M.; Enck, R. C. Onsager mechanism of photogeneration in amorphous selenium. *Phys. Rev. B* **1975**, 11, 5163-5174.
[43] Haastrup, S.; Latini, S.; Bolotin, K.; Thygesen, K. S. Stark shift and electric-field-induced dissociation of excitons in monolayer MoS_2 and hBN/MoS_2 heterostructures. *Phys. Rev. B* **2016**, 94, 041401.
[44] Radisavljevic, B.; Radenovic, A.; Brivio, J.; Giacometti, V.; Kis, A. Single-layer MoS_2 transistors. *Nat. Nanotechnol*. **2011**, 9, 147-150.
[45] Dumcenco, D.; Ovchinnikov, D.; Marinov, K.; Lazic, P.; Gibertini, M.; Marzari, N.; Sanchez, O. L.; Kung, Y.-C. Krasnozhon, D.; Chen, M.-W.; Bertolazzi, S.; Gillet, P.; i Morral, A. F.; Radenovic, A.; Kis, A. Large-area epitaxial monolayer MoS_2. *ACS Nano* **2015**, 9, 4611-4620.